Published in final edited form as:
J Cell Physiol. 2014 November ; 229(11): 1822–1830. doi:10.1002/jcp.24636.

Probiotic *L. reuteri* treatment prevents bone loss in a menopausal ovariectomized mouse model

Robert A. Britton[3,*], **Regina Irwin**[1], **Darin Quach**[3], **Laura Schaefer**[3], **Jing Zhang**[1], **Taehyung Lee**[1], **Narayanan Parameswaran**[1], and **Laura R. McCabe**[1,2,4,*]

[1]Michigan State University, Department of Physiology, East Lansing, MI 48824

[2]Michigan State University, Department of Radiology, East Lansing, MI 48824

[3]Michigan State University, Department of Microbiology and Molecular Genetics, East Lansing, MI 48824

[4]Michigan State University, Biomedical Imaging Research Center, East Lansing, MI 48824

Abstract

Estrogen deficiency is a major risk factor for osteoporosis that is associated with bone inflammation and resorption. Half of women over the age of 50 will experience an osteoporosis related fracture in their lifetime, thus novel therapies are needed to combat post-menopausal bone loss. Recent studies suggest an important role for gut-bone signaling pathways and the microbiota in regulating bone health. Given that the bacterium *Lactobacillus reuteri* ATCC PTA 6475 (*L. reuteri*) secretes beneficial immunomodulatory factors, we examined if this candidate probiotic could reduce bone loss associated with estrogen deficiency in an ovariectomized (Ovx) mouse menopausal model. Strikingly, *L. reuteri* treatment significantly protected Ovx mice from bone loss. Osteoclast bone resorption markers and activators (Trap5 and RANKL) as well as osteoclastogenesis are significantly decreased in *L. reuteri* treated mice. Consistent with this, *L. reuteri* suppressed Ovx-induced increases in bone marrow CD4+ T-lymphocytes (which promote osteoclastogenesis) and directly suppressed osteoclastogenesis in vitro. We also identif ied that *L. reuteri* treatment modifies microbial communities in the Ovx mouse gut. Together, our studies demonstrate that *L. reuteri* treatment suppresses bone resorption and loss associated with estrogen deficiency. Thus, *L. reuteri* treatment may be a straightforward and cost-effective approach to reduce post-menopausal bone loss.

Keywords

menopause; osteoporosis; probiotics; osteoclast; intestine; gut

[*]Editorial correspondence and reprint requests to: Laura R. McCabe, Ph.D., Michigan State University, Departments of Physiology and Radiology, 2201 Biomedical Physical Science Bldg., East Lansing, MI 48824, (517) 884-5152, (517) 355-5125 FAX, mccabel@msu.edu, Robert Britton, Ph.D., Michigan State University, Department of Microbiology and Molecular Genetics 6175 Biomedical Physical Science Bldg., East Lansing, MI 48824, 517-884-5395, rbritton@msu.edu.

All authors state that they have no conflict of interest.

Introduction

Finding effective novel treatments for bone loss is a priority, since it is estimated that by 2020 more than 61 million women and men will have osteoporosis (National-Osteoporosis-Foundation, 2009). Menopause is a major risk factor for osteoporosis. In fact, one in two women over the age of 50 will experience an osteoporosis related fracture in their lifetime. Estrogen deficiency in post-menopausal women promotes bone loss, increases bone resorption and enhances fracture risk (ESHRE Capri Workshop Group 2010; Manolagas, 2010; McNamara, 2010; Riggs et al., 2002). Similarly, ovariectomy (Ovx) depletes estrogen in mice leading to bone loss at multiple skeletal sites and increased bone turnover (Bouxsein et al., 2005; Li et al., 2011). Bone loss ensues due to a greater increase in bone resorption compared to bone formation (Jilka et al., 1998; Li et al., 2011). Studies demonstrate that bone inflammation is increased with estrogen deficiency and is linked to osteoclastogenesis and hence bone resorption (Jilka et al., 1998; Li et al., 2011; Manolagas, 2010). Despite all of the current treatments available for promoting bone health, the number of osteoporotic patients is on the rise in the U.S. and worldwide. A lack of awareness that one is at risk early in life, an increasing elderly population, and patient noncompliance due to unwanted medication side effects are likely contributors to this outcome. In addition, conventional bone loss treatments are not always effective. Therefore, new approaches to increase bone density are needed.

The role of the intestinal microbiota in regulating human health and disease is receiving increasing attention (Backhed et al., 2012; Lemon et al., 2012). While the intestine is known to be key for calcium and vitamin D metabolism, the effect of bacterial community changes on bone health, especially in estrogen deficiency, has not been thoroughly examined. Reports have indicated that prebiotics (non-digestible polysaccharides that modulate gut microbial composition) can increase bone density (Abrams et al., 2005; Coxam, 2007; Roberfroid et al., 2002; Weaver et al., 2011; Yang et al., 2012) especially in combination with probiotics (Scholz-Ahrens and Schrezenmeir, 2007). Probiotics (microorganisms that provide health benefit to the host when ingested in adequate amounts) have also been shown to increase cortical bone thickness in chicken (Mutus et al., 2006) as well as reduce bone loss in aging mice (Kimoto-Nira et al., 2007) and improve bone density in male mice (McCabe et al., 2013). More recently, studies indicate that germ free mice have greater bone density compared to mice harboring a conventional microbiota, further supporting a link between the intestine and bone (Sjogren et al., 2012). The mechanistic basis by which the gut and the intestinal microbiota regulate bone density, however, is not known.

Lactobacillus reuteri is an established probiotic species that has proven beneficial in clinical trials (Shornikova et al., 1997; Tubelius et al., 2005; Weizman et al., 2005). *L. reuteri* is one of a handful of lactobacilli indigenous to the human and mouse GI tract (Reuter, 2001; Valeur et al., 2004) and has never been associated with causing disease. *L. reuteri* ATCC PTA 6475 produces antimicrobial compounds such as reuterin (Schaefer et al., 2010) as well as molecules that have potent anti-TNF activity *in vitro* (Thomas et al., 2012). Previously we identified that *L. reuteri* 6475 improves bone density in male mice (McCabe et al., 2013). Therefore we hypothesized that *L. reuteri* 6475 could modulate the intestinal microbiota and/or regulate systemic and bone inflammation, resulting in suppressed bone loss in Ovx

mice. Consistent with our premise, *L. reuteri* treatment prevents Ovx-induced bone loss thereby implicating probiotic ingestion as a straightforward and cost-effective approach to prevent menopause-induced bone loss.

Materials and Methods

Experimental design

Balb/c mice 12 weeks of age non-Ovx and Ovx were obtained from Harlan Laboratories (Indianapolis, IN). Mice were allowed to acclimate to animal room for one-week prior to start of experiment. After one week, mice were treated by gavaging with 300μl (1×10^9 cfu/ml) with *L. reuteri* ATCC PTA 6475 or MRS broth, (vehicle control) three times per week for four weeks and *L. reuteri* was also added to the drinking water at a concentration of 1.5×10^8 cfu/ml unless otherwise noted in the figure legend. Mice were given Teklad 2019 chow (Madison, WI) and water ad libitum and were maintained on a 12 hour light/dark cycle. Food and water intake were monitored and did not differ between groups (data not shown). All animal procedures were approved by the Michigan State University Institutional Animal Care and Use Committee.

μCT bone imaging

Fixed femurs were scanned using a GE Explore Locus microcomputed tomography (μCT) system at a voxel resolution of 20 μm obtained from 720 views. Beam angle of increment was 0.5, and beam strength was set at 80 peak kV and 450 uA. Each run consisted of control (non-Ovx) and Ovx and Ovx + *L. reuteri* treated mouse bones, and a calibration phantom to standardize grayscale values and maintain consistency. On the basis of autothreshold and isosurface analyses of multiple bone samples, a fixed threshold (760) was used to separate bone from bone marrow. Bone measurements were blinded; thus, knowledge of what mouse condition the analyzed bone was from was unknown until the final data was pooled. Trabecular bone analyses were performed in a region of trabecular bone defined at 1% of the total length (~0.17 mm) proximal to the growth plate of and extending 2 mm toward the diaphysis excluding the outer cortical bone. Trabecular bone mineral content, bone volume fraction, thickness, spacing, and number values were computed by a GE Healthcare MicroView software application for visualization and analysis of volumetric image data. Cortical measurements were performed in a 2 X 2 X 2 mm cube centered midway down the length of the bone using a threshold of 1000 to separate bone from marrow.

Femur histomorphometry and dynamic measures

Femurs were fixed in 10% formalin and transferred to 70% ethanol after 24 hours. Fixed samples were processed on an automated Thermo Electron Excesior tissue processor for dehydration, clearing, and infiltration using a routine overnight processing schedule. Samples were then embedded in Surgipath-embedding paraffin on a Sakura Tissue Tek II-embedding center. Paraffin bocks were sectioned at 5 μm on a Reichert Jung 2030 rotary microtome. Slides were stained for TRAP activity and counterstained with hematoxylin according to manufacturer protocol (387A-1KT, Sigma, St. Louis, MO). Osteoblast and osteoclast surface area was measured and expressed as a percentage of total bone surface in the femur trabecular region ranging from the growth plate to 2 mm distal.

For dynamic histomorphometric measures of bone formation, mice were injected intraperitoneally with 200μl of 10mg/ml calcein (Sigma, St. Louis, MO, USA) dissolved in sterile saline at 7 and 2 days prior to harvest. L3-L4 vertebrae were fixed in formalin at time of harvest then transferred to 70% ethanol 48 hours later. Vertebrae were then embedded, sectioned and examined under UV light. Five images were taken and the distance between the calcein lines (bone formation rate, BFR) and their length along the bone surface was measured and used to calculate mineral apposition rate (MAR).

Bone RNA analysis

Immediately following euthanasia tibias were cleaned of muscle and connective tissue, snap frozen in liquid nitrogen and stored at -80°C. Frozen tibias were crushed under liquid nitrogen conditions with a Bessman Tissue Pulverizer (Spectrum Laboratories, Rancho Dominguez, CA). RNA was isolated using TriReagent (Molecular Research Center, Cincinnati, OH), and integrity assessed by formaldehyde-agarose gel electrophoresis. cDNA was synthesized by reverse transcription using Superscript II Reverse Transcriptase Kit and oligo dT(12-18) primers (Invitrogen, Carlsbad, CA) and amplified by real-time PCR with iQ SYBR Green Supermix (BioRad, Hercules, CA), and gene specific primers were synthesized by Integrated DNA Technologies (Coralville, IA). Hypoxanthine guanine phosphoribosyl transferase (HPRT) mRNA levels do not fluctuate with Ovx were used as an internal control. Amplicon specificity was confirmed by melting curve, size, and sequence analysis. Primers for real-time PCR were designed or previously described: osteocalcin, Trap5b and HPRT(Harris et al., 2009). Receptor activator of nuclear factor kappa-B ligand (RANKL) was amplified using 5′ -TTT GCA GGA CTC GAC TCT GGA G-3′ and 5′ -TCC CTC CTT TCA TCA GGT TAT GAG-3′ (Zhao et al., 2002)(Motyl and McCabe, 2009). Osterix was amplified using 5’-CCC TTC TCA AGC ACC AAT GG-3’ and 5’AGG GTG GGT AGT CAT TTG CAT AG-3’ (Jadlowiec et al., 2004). Real time PCR was carried out for 40 cycles using the iCycler (Bio-Rad) and data were evaluated using the iCycler software. Each cycle consisted of 95°C for 15 s, 60°C for 30 s (except for osteocalcin which had an annealing temperature of 65°C), and 72°C for 30 s. cDNA-free samples, a negative control, did not produce amplicons. Melting curve and gel analyses (sizing, isolation, and sequencing) were used to verify single products of the appropriate base pair size.

Serum Measurements

Blood was collected at the time of harvest, allowed to clot at room temperature for 5 minutes, then centrifuged at 4,000 rpm for 10 minutes. Serum was removed, frozen in liquid nitrogen and stored at -80°C. Serum went through no more than two freeze/thaw cycles. Serum TRAP5b and Osteocalcin were measured using a Mouse TRAP and OC assay kits (SB-TR103, Immunodiagnostic Systems Inc., Fountain Hills, AZ, USA and BT-470, Biomedical Technologies Inc., Stoughton, MA, USA respectively) according to the manufacturer’s protocol.

Bacterial strains and culture

L. reuteri ATCC PTA 6475 was cultured under anaerobic conditions in deMan, Rogosa, Sharpe media (MRS, Difco) for 16-18 hours at 37C. On the following day, the overnight

culture was sub-cultured into fresh MRS and grown until log phase (OD_{600} = 0.4). Cells are harvested by centrifugation at 4000 rpm for 10 minutes. Minimum Essential Medium (MEMα, Invitrogen) conditioned medium was generated by resuspending the bacterial pellet in pre-warmed MEMα and incubating with gentle shaking at 37°C for 3h. Cells were harvested and the supernatant is separated from the bacterial cell pellet, pH neutralized, and filter-sterilized using PVDF membrane filters (0.22μm pore size, Millipore). An equivalent of OD_{600}= 1.0 was lyophilized for long-term storage at -80°C.

FACS analysis

After the appropriate time points of *L. reuteri*/OVX treatment, bone marrow cells were collected and cells were stained for various immune cell populations as described(Fukata et al., 2008) (Patial et al., 2011). Stained cells were analyzed in Flow cytometry and gated for various populations using FlowJo software, as described before (Lee et al., 2013).

Osteoclast Generation and Characterization

For primary osteoclastogenesis assays, bone marrow cells were flushed from mouse femurs and plated at 900,000 cells per 24 well. Flushed cells were fed with αMEM (Invitrogen) containing 10% FBS (Atlanta Biologicals) and were treated with 2 ng/ml RANKL (R&D Systems) and 30 ng/ml M-CSF (R&D Systems) to induce osteoclastogenesis. The bone marrow cells were allowed to grow undisturbed for 4 days at which point they were fed with the complete media above. Twenty-four hours later cells were stained for tartrate-resistant acid phosphatase (TRAP) (Sigma). Cells were examined by microscopy and photographed (5 fields per well) and multinucleated cells that stained TRAP positive were counted and averaged per condition.

Raw 264.7 cells, a murine macrophage cell line, were obtained from ATCC and maintained in phenol red-free MEMα and charcoal-stripped fetal bovine serum (Invitrogen) at 37°C with 5% CO_2. In 12-well tissue culture plates (Costar), 100,000 cells/well were seeded. On the following day, cells were washed with PBS and then stimulated with RANKL (100 ng/ml) and M-CSF (10 ng/ml). At this time, lyophilized *L. reuteri* MEMα conditioned medium was re-solubilized in culture medium and added to the cells. The medium and *L. reuteri* MEMα conditioned medium were replaced on days 3 and 5. At day 6, cells were fixed and stained for tartrate-resistant acid phosphatase (TRAP) according to manufacturer's protocol (Sigma cat no. 387A). Multinucleated giant cells that stained for TRAP were considered osteoclasts.

DNA preparation of tissue samples

Intestinal tissue samples were transferred to Mo Bio Ultra Clean Fecal DNA Bead Tubes (MoBio) containing 360μl Buffer ATL (Qiagen) and homogenized for one minute in a a BioSpec Mini-Beadbeater. 40μl Proteinase K (Qiagen) was added and samples were incubated for 30 minutes at 55°C, homogenized again for one minute, and incubated at 55°C for an additional 30 minutes. DNA was extracted with the Qiagen DNeasy Blood and Tissue kit.

PCR amplification for beta diversity analysis

Bacterial 16S sequences spanning variable regions V4-V6 were amplified by PCR from intestinal DNA using barcoded V4-V6 primers designed by the Human Microbiome Project. 20μl reactions for each sample were prepared in triplicate and contained 0.75 units Accuprime High Fidelity Taq DNA polymerase (Invitrogen), 1X Accuprime PCR Buffer II (Invitrogen), 0.4μM primers, and 400μg DNA. Reactions were performed in an Eppendorf Pro thermal cycler with 3 minutes at 94°C followed by 30 cycles of 94°C × 30 sec, 60°C × 45 sec, 72°C × 2min. Triplicate reactions were then pooled, purified using Agencourt AMPure XP magnetic beads (Beckman Coulter), and quantified using the QuantIt High Sensitivity DNA assay kit (Invitrogen).

454 sequencing and analysis

Sequencing was performed on a Roche 454 GS Junior Sequencer using Roche's GS Junior Titanium EmPCR Lib-L kit and Titanium Sequencing kit. Sequences were processed for analysis using the mothur software package version 1.21 (Schloss et al., 2009) using the Schloss laboratory standard operating procedure available on the mothur Wiki website (http://www.mothur.org/wiki/). A total of 71,061 quality bacterial 16S sequences (median 3773 sequences per sample) were obtained from mouse jejunum samples and 82,903 sequences (median 3875 sequences per sample) were obtained from ileum samples. Of these sequences, 96.2% in jejunum/90% in ileum were classified as belonging to the Proteobacteria, Firmicutes, or Bacteroidetes phyla. Rare OTUs occurring 1 or 2 times across the data set were removed to minimize bias due to sequencing error. To minimize bias due to uneven sequencing depth across samples, randomly selected subsets of 600 sequences per sample in jejunum/1000 sequences per sample in ileum were generated in mothur to calculate operational taxonomic units (OTU) at 97% similarity. *L. reuteri* 6475 was not detected in the communities. Species richness measurements for Chao1 (Chao, 1984; Chao and Lee, 1992) for each sample were calculated in mother on 12 independent subsamplings for each sample, averaged, and tested for statistically significant differences between the experimental groups using analysis of variance (ANOVA) and Tukey's range test in the PAST software package (Hammer, Ø., Harper, D.A.T., and P. D. Ryan, 2001. PAST: Paleontological Statistics Software Package for Education and Data Analysis. Palaeontologia Electronica 4(1): 9pp.). Beta diversity analysis was performed using mothur and PAST and visualized using PCoA plots generated in R (R Development Core Team, 2011). R: A language and environment for statistical computing. R Foundation for Statistical Computing, Vienna, Austria. ISBN 3-900051-07-0, URL http://www.R-project.org/). Taxonomic classification was performed using RDP Classifier (Wang et al., 2007). SIMPER analyses in PAST and PCoA analyses in R were performed to identify OTUs that contributed to microbial community differences between the experimental groups.

Statistical analysis

All measurements are presented as the mean ± SE or SD as noted. ANOVA was performed followed by post hoc analysis (Tukey) when results of of ANOVA indicated significance ($\alpha \leq 0.05$).

Results

The effect of probiotic ingestion, specifically *L. reuteri* 6475, on ovariectomized (Ovx)-induced bone loss was examined in 12-week old Balb/c mice. One week after ovariectomy the mice were treated with *L. reuteri* 6475 or vehicle (broth) 3 times a week. After 4 weeks, microcomputed tomography was used to assess bone loss at two sites, femur and vertebrae. As expected, the trabecular bone of the Ovx mouse distal femur and L3 vertebrae displayed a bone volume loss (50 and 25%, respectively; Figure 1B). *L. reuteri* treatment of Ovx mice, on the other hand, completely prevented femur and vertebral trabecular bone volume loss resulting in a BV/TV similar to control mice (Figure 1B). Other trabecular parameters of the femoral and vertebral regions, which were negatively affected by Ovx (trabecular thickness, number and spacing), were also protected by *L. reuteri* treatment (Tables 1 and 2). On the other hand, femoral diaphysis cortical bone parameters did not display a large enough change to be significant in Ovx mice (Table 1). Treatment of sham-operated female mice had no effect on trabecular bone volume (Figure 1C) consistent with our previous report (McCabe et al., 2013).

To identify the effect of *L. reuteri* 6475 treatment on bone remodeling, we examined both osteoblast and osteoclast parameters in 3-week post-Ovx mice. We identified that 2-weeks of *L. reuteri* treatment was able to prevent Ovx-induced increases in bone mRNA levels of RANKL, an osteoclastogenesis activator cytokine (Figure 2A). Probiotic treatment also reduced bone TRAP5 mRNA levels, an osteoclast marker (Figure 2A). Serum TRAP5 levels were modestly decreased in the *L. reuteri* treated Ovx mice (data not shown). To further assess if osteoclastogenesis is altered, femur marrow cells were obtained from mice in each group and cultured to stimulate osteoclast differentiation. While cells obtained from Ovx mice displayed increased osteoclastogenesis, cells obtained from Ovx mice treated with *L. reuteri* were similar to controls (Figure 2B). Taken together, these results suggest that *L. reuteri* suppresses osteoclast activity in this mouse model. We did not observe differences in any osteoblast parameters among conditions after treatment (Figure 2C).

We further examined dynamic and static osteoblast parameters at the 4-week *L. reuteri* treatment time point (in mice more than 4 months old at this time). However, at this point we did not observe significant differences between control and Ovx mice or *L. reuteri* treated Ovx mice. Specifically, the level of bone formation rate, osteoblast surface or tibial osteocalcin and osterix mRNA did not differ between any of the three conditions (Figure 3). Similarly, osteoclast parameter markers did not differ among the groups at this time point (Figure 3). This is likely due to changes in osteoclastogenesis having already occurred by 5 weeks after ovariectomy. However, note that tibial RANKL RNA levels displayed a trend to increase with Ovx and a decrease in Ovx mice treated with *L. reuteri*, which is consistent with the 2-week treatment time point.

Utilizing these animals harvested after treatment with *L. reuteri* for two weeks we examined the influence of *L. reuteri* on bone marrow CD4+ T cells, which are known to affect osteoclast activity (Li et al., 2011). As shown in Figure 4, there was a significant increase in the percentage of $CD4^+$ T-cells in Ovx mice compared to controls. Treatment with *L. reuteri* caused significant decrease in CD4+ T-lymphocytes (compared to Ovx mice). These

changes suggest that *L. reuteri* 6475 could be reducing osteoclastogenesis through suppression of osteoclast inducing signals from T-cells.

Because *L. reuteri* could directly affect the intestinal microbiota, we assessed alterations in intestinal microbial diversity since the microbiota could contribute to changes in intestinal function, immune function and possibly bone density (Sjogren et al., 2012). Samples from *L. reuteri* 6475-treated mice had significantly higher measurements of richness than those from non-treated mice, including Chao 1 estimate values (ANOVA $p<0.0023$) and ACE richness values (ANOVA $p<0.0014$). Analysis of the jejunum samples using diversity metrics that utilize only species richness (Jaccard) or richness and evenness (Bray-Curtis) showed statistically significant separation between the three communities, non Oxx, Ovx, and Ovx + *L. reuteri* (Bray-Curtis $R= 0.34$, $p <0.018$, Jaccard $R = 0.42$, $p < 0.0004$; Figure 5). Pairwise comparisons demonstrated that although Ovx did not significantly alter microbial community structure compared to non-Ovx animals; treating animals with *L. reuteri* resulted in a significant change in jejunal communities compared with wild-type and Ovx animals (Table 3, Figure 5). We also identified operational taxonomic units (OTUs) that were associated with differences between these communities and found that several OTUs classified as *Clostridiales* were significantly more abundant in *L. reuteri* treated animals than in non-treated animals. Conversely, we found that several OTUs classified as *Bacteriodales* trended towards being decreased in *L. reuteri* treated Ovx animals compared to untreated Ovx and non-Ovx controls. Similar changes in microbial diversity were observed in the ileum (data not shown). Thus, we have uncovered profound shifts in specific members in microbial communities that are associated with the suppression of bone loss by *L. reuteri* 6475.

Finally, to address the possibility that *L. reuteri* 6475 could be directly affecting bone resorption by producing a factor that affects osteoclastogenesis, we induced osteoclast formation in a murine macrophage cell line in the presence or absence of *L. reuteri* 6475 conditioned medium. While control cultures and vehicle treated cultures displayed active osteoclastogenesis marked by the presence of many large multinucleated, TRAP5 positive cells, the presence of *L. reuteri* supernatant in the culture prevented RANKL and M-CSF induced osteoclastogenesis by 70% (Figure 6). This indicates that *L. reuteri* 6475 secretes a soluble factor capable of directly suppressing osteoclast formation *in vitro*.

Discussion

Probiotics are increasingly being used worldwide to treat health problems. Studies indicate that probiotics may be effective in the treatment of some gastrointestinal diseases such as colic, irritable bowel and inflammatory bowel disease (Thomas and Greer, 2010; Whelan and Quigley, 2013). In addition, probiotics have also showed promise in ameliorating other ailments that are distal to the gut, including eczema, asthma, and allergies (Yan and Polk, 2011; Yoo et al., 2007). Our studies demonstrate that oral administration of the candidate probiotic *L. reuteri* 6475 can enhance bone health under estrogen deficiency conditions. Benefits were observed in both the appendicular and axial skeleton, indicating a broad ranging bone effect. Furthermore, *L. reuteri* 6475 treatment of Ovx mice restored all trabecular bone parameters.

Previous work has indicated that the intestinal microbiota may impact bone health. Rodents and birds treated with prebiotics, such as inulin, oligofructose and galactooligosaccharides, can also display increased bone density (Abrams et al., 2005; Coxam, 2007; Roberfroid et al., 2002; Scholz-Ahrens and Schrezenmeir, 2007; Weaver et al., 2011; Yang et al., 2012). For example, galactooligosaccharide intake resulted in a dose dependent increase in rat femur trabecular bone volume (Weaver et al., 2011). However, inulin treatment had no effect on bone parameters in pigs (Jolliff and Mahan, 2012). Interestingly, some studies demonstrate that prebiotic treatment can increase the presence of bifidobacteria in the stool (Weaver et al., 2011), but the direct role of this bacterial genus and whether osteoblast or osteoclast activity was affected was not determined. A few studies have examined the role of probiotic treatment on bone and show increased bone density, but also do not show how treatment affects bone remodeling (Kimoto-Nira et al., 2007; Mutus et al., 2006).

Does *L. reuteri* 6475 affect anabolic and/or catabolic bone remodeling pathways? Identifying changes in osteoclast and osteoblast activities in our study proved somewhat difficult. We did not observe large differences in bone remodeling parameters between non-Ovx and Ovx mice at 2 or 4 weeks of age. This may be due to the use of adult mice (which we felt was most applicable to estrogen deficient women) rather than preadolescent mice, which have a faster rate of bone growth/remodeling and may more readily display changes (but are also growing). However, one common finding was that *L. reuteri* 6475 reduced Ovx mouse Trap5 and RANKL bone RNA levels at 2 and 4 weeks post-treatment. It may be that RNA levels provide the greatest detection sensitivity in our model. Further in vitro studies will help delineate whether *L. reuteri* affects RANKL production from T-cells or osteoblasts or both. Alternatively, *L. reuteri* might decrease the number of osteoclastogenic T-cells in the marrow. Consistent with this, marrow CD4+ T cells, which have been shown to be important mediators of osteoclastogenesis in estrogen deficiency (reviewed in (Pacifici, 2012), were significantly decreased in the presence of *L. reuteri* 6475. At least two mechanisms have been proposed as to how T-cells might mediate OVX-induced bone loss. While one involves direct activation of T-cells and production of TNFα, the other involves activation of stromal cells by T-cells to produce osteoclastogenic cytokines leading to enhanced bone loss. Future studies will determine whether a specific TNFα-producing T-cell population is also decreased by LR in OVX mice. Compared to the changes in CD4+ T cells, CD8+ T cells decreased in Ovx mice and increased in response to probiotic treatment. Future studies will examine whether other immune cell populations (relevant to osteoclastogenesis) in the bone marrow and other systemic sites are also modulated by probiotic treatment and how these changes affect bone health.

Consistent with these in vivo results, our in vitro osteoclastogenesis experiments demonstrate a potential direct role of *L. reuteri* 6475 in decreasing osteoclast activity because the medium of *L. reuteri* cultures is capable of suppressing osteoclast differentiation in a cell culture model of osteoclastogenesis. This cannot be attributed to any pH effect since the medium was neutralized prior to treating the cells. *L. reuteri* is known to secrete a variety of factors including the antimicrobial reuterin (Schaefer et al., 2010) and molecules that reduce TNFα activity *in vitro* (Thomas et al., 2012). The latter could be a key factor in the response that we see *in vitro* since TNFα stimulates bone resorption (Teitelbaum, 2007).

Such a factor could also cross the gut epithelium and affect local, systemic and bone marrow immune responses and/or have direct effects on osteoclasts. In addition, we have reported that L. reuteri ATCC PTA 6475 produces histamine, which contributes to one of the immunomodulatory activities exhibited by *L. reuteri* ATCC PTA 6475. Specifically, L. reuteri production of histamine can suppress TNF signaling through modulation of PKA and ERK signaling (Thomas et al., 2012) providing a mechanistic link between this probiotic, TNF signaling suppression and the prevention of Ovx induced bone loss. Future mechanistic studies deleting the expression of these molecules such as reuterin or histamine production will test their role in *L. reuteri's* bone benefits. Regardless of the mechanism, the fact that markers of osteoclastogenesis as well as cells important in osteoclastogenesis, are modulated by *L. reuteri* 6475 demonstrates important role for probiotics in this estrogen-deficiency model of bone loss.

Interestingly, we did not observe any *L. reuteri* induced change in osteoblast activity/ markers at the time points we studied. This is in contrast to studies in male mice (bred under pathogen free conditions), which display an anabolic response to *L. reuteri* 6475 that is characterized by increased bone formation rate and osteoblast markers (McCabe et al., 2013). It may be that we were not at the optimal time point to detect a bone formation response in the treated Ovx mice. A variety of factors could contribute to gender differences including different gut microbiomes, bone remodeling rates, immunoresponsiveness and/or composition of marrow immune cells that can affect bone formation and resorption (Li et al., 2011).

One possible indirect mechanism by which *L. reuteri* 6475 could impact the suppression of bone loss in Ovx animals is by alteration of the immune response by changing intestinal microbial communities found in Ovx animals. Dysbiosis of gut communities can promote or exacerbate diseases including obesity, diabetes and IBD (Kuhbacher et al., 2006; Oakley et al., 2008; Sartor, 2008; Vaarala et al., 2008; Wen et al., 2008) while alterations in the host immune system can also modify the structure and function of the intestinal microbiota to promote disease. Interestingly, bone density can be enhanced by the absence of luminal bacteria (Sjogren et al., 2012). This underlies that the gut microbiota (greater than 1000 species composition) comprises a community of microbes that promotes health, but that there is a cost to having these microbes in such close association with us. Given that the absence of gut bacteria is beneficial to bone, gut bacteria in a standard mouse likely has an overall negative effect on bone health that may be overcome by ingestion of *L. reuteri* 6475. Consistent with this we found significant changes in microbial communities upon *L. reuteri* 6475 treatment of Ovx animals in the small intestine when compared to Ovx and non-Ovx control communities. Interestingly, several OTUs that were classified as Clostridiales are the main groups of bacteria that are driving the separation of the L. reuteri treated Ovx communities from the other two groups. Interestingly, several murine clostridia have been implicated in the regulation of the immune system by driving the upregulation of colonic T_{reg} cells (Atarashi et al., 2011), and thus an increase in this bacterial class may be directly linked to anti-inflammatory effects in the bone. At this point these are associations between microbial communities and bone health and we are actively pursuing if the microbiota plays a direct role in Ovx mediated bone loss.

Taken together, *L. reuteri* 6475 treatment can benefit bone health in estrogen deficient mice. We demonstrate a role for this probiotic in the suppression of osteoclast activity, which is known to increase with estrogen deficiency. The idea of a natural product for the treatment of menopause-induced osteoporosis is appealing since existing therapies have side effects. Future studies looking at the long term impact of probiotic treatment on gut and bone health, as well as probiotic treatment after well established osteopenia, will be important for providing clinically relevant insight into treating menopause induced bone loss. Importantly, our studies also warrant future mechanistic research in this exciting area utilizing gastrointestinal health to treat bone disease.

Acknowledgments

The authors thank the Investigative Histology Laboratory in the Department of Physiology, Division of Human Pathology and the Biomedical Imaging Center at Michigan State University for their assistance with histology and imaging, respectively. These studies were supported by funding from the National Institute of Health, National Center for Complementary and Alternative Medicine (R21-RAT005472 and 1RO1AT007695), Biogia, and by a Strategic Partnership Grant from Michigan State University.

Funded by grants from NIH NCAAM (AT005472), MSU and Biogia to LRM and RAB and by NIH NCAAM (1RO1AT007695) to LRM, RAB and NP

References

ESHRE Capri Workshop Group. Bone fractures after menopause. Hum Reprod Update. 2010; 16(6): 761–773. [PubMed: 20427370]

Abrams SA, Griffin IJ, Hawthorne KM, Liang L, Gunn SK, Darlington G, Ellis KJ. A combination of prebiotic short- and long-chain inulin-type fructans enhances calcium absorption and bone mineralization in young adolescents. The American journal of clinical nutrition. 2005; 82(2):471–476. [PubMed: 16087995]

Atarashi K, Tanoue T, Shima T, Imaoka A, Kuwahara T, Momose Y, Cheng G, Yamasaki S, Saito T, Ohba Y, Taniguchi T, Takeda K, Hori S, Ivanov II, Umesaki Y, Itoh K, Honda K. Induction of colonic regulatory T cells by indigenous Clostridium species. Science. 2011; 331(6015):337–341. [PubMed: 21205640]

Backhed F, Fraser CM, Ringel Y, Sanders ME, Sartor RB, Sherman PM, Versalovic J, Young V, Finlay BB. Defining a healthy human gut microbiome: current concepts, future directions, and clinical applications. Cell host & microbe. 2012; 12(5):611–622. [PubMed: 23159051]

Bouxsein ML, Myers KS, Shultz KL, Donahue LR, Rosen CJ, Beamer WG. Ovariectomy-induced bone loss varies among inbred strains of mice. J Bone Miner Res. 2005; 20(7):1085–1092. [PubMed: 15940361]

Chao A. Nonparametric-Estimation of the Number of Classes in a Population. Scand J Stat. 1984; 11(4):265–270.

Chao A, Lee SM. Estimating the Number of Classes Via Sample Coverage. J Am Stat Assoc. 1992; 87(417):210–217.

Coxam V. Current data with inulin-type fructans and calcium, targeting bone health in adults. The Journal of nutrition. 2007; 137(11 Suppl):2527S–2533S. [PubMed: 17951497]

Fukata M, Breglio K, Chen A, Vamadevan AS, Goo T, Hsu D, Conduah D, Xu R, Abreu MT. The myeloid differentiation factor 88 (MyD88) is required for CD4+ T cell effector function in a murine model of inflammatory bowel disease. J Immunol. 2008; 180(3):1886–1894. [PubMed: 18209086]

Harris L, Senagore P, Young VB, McCabe LR. Inflammatory bowel disease causes reversible suppression of osteoblast and chondrocyte function in mice. American journal of physiology Gastrointestinal and liver physiology. 2009; 296(5):G1020–1029. [PubMed: 19299577]

Jadlowiec J, Koch H, Zhang X, Campbell PG, Seyedain M, Sfeir C. Phosphophoryn regulates the gene expression and differentiation of NIH3T3, MC3T3-E1, and human mesenchymal stem cells via the

integrin/MAPK signaling pathway. The Journal of biological chemistry. 2004; 279(51):53323–53330. [PubMed: 15371433]

Jilka RL, Takahashi K, Munshi M, Williams DC, Roberson PK, Manolagas SC. Loss of estrogen upregulates osteoblastogenesis in the murine bone marrow. Evidence for autonomy from factors released during bone resorption. The Journal of clinical investigation. 1998; 101(9):1942–1950. [PubMed: 9576759]

Jolliff JS, Mahan DC. Effect of dietary inulin and phytase on mineral digestibility and tissue retention in weanling and growing swine. J Anim Sci. 2012; 90(9):3012–3022. [PubMed: 22665666]

Kimoto-Nira H, Suzuki C, Kobayashi M, Sasaki K, Kurisaki J, Mizumachi K. Anti-ageing effect of a lactococcal strain: analysis using senescence-accelerated mice. Br J Nutr. 2007; 98(6):1178–1186. [PubMed: 17617939]

Kuhbacher T, Ott SJ, Helwig U, Mimura T, Rizzello F, Kleessen B, Gionchetti P, Blaut M, Campieri M, Folsch UR, Kamm MA, Schreiber S. Bacterial and fungal microbiota in relation to probiotic therapy (VSL#3) in pouchitis. Gut. 2006; 55(6):833–841. [PubMed: 16401690]

Lee T, Lee E, Irwin R, Lucas PC, McCabe LR, Parameswaran N. beta-arrestin-1 deficiency protects mice from experimental colitis. The American journal of pathology. 2013; 182(4):1114–1123. [PubMed: 23395087]

Lemon KP, Armitage GC, Relman DA, Fischbach MA. Microbiota-targeted therapies: an ecological perspective. Science translational medicine. 2012; 4(137):137rv135.

Li JY, Tawfeek H, Bedi B, Yang X, Adams J, Gao KY, Zayzafoon M, Weitzmann MN, Pacifici R. Ovariectomy disregulates osteoblast and osteoclast formation through the T-cell receptor CD40 ligand. Proceedings of the National Academy of Sciences of the United States of America. 2011; 108(2):768–773. [PubMed: 21187391]

Manolagas SC. From estrogen-centric to aging and oxidative stress: a revised perspective of the pathogenesis of osteoporosis. Endocr Rev. 2010; 31(3):266–300. [PubMed: 20051526]

McCabe LR, Irwin R, Schaefer L, Britton RA. Probiotic use decreases intestinal inflammation and increases bone density in healthy male but not female mice. J Cell Physiol. 2013; 228(8):1793–1798. [PubMed: 23389860]

McNamara LM. Perspective on post-menopausal osteoporosis: establishing an interdisciplinary understanding of the sequence of events from the molecular level to whole bone fractures. J R Soc Interface. 2010; 7(44):353–372. [PubMed: 19846441]

Motyl K, McCabe LR. Streptozotocin, Type I Diabetes Severity and Bone. Biol Proced Online. 2009

Mutus R, Kocabagli N, Alp M, Acar N, Eren M, Gezen SS. The effect of dietary probiotic supplementation on tibial bone characteristics and strength in broilers. Poultry science. 2006; 85(9):1621–1625.

National-Osteoporosis-Foundation. National Osteoporosis Foundation National Web Site. 2009. http://www.nof.org/

Oakley BB, Fiedler TL, Marrazzo JM, Fredricks DN. Diversity of human vaginal bacterial communities and associations with clinically defined bacterial vaginosis. Appl Environ Microbiol. 2008; 74(15):4898–4909. [PubMed: 18487399]

Pacifici R. Role of T cells in ovariectomy induced bone loss--revisited. J Bone Miner Res. 2012; 27(2):231–239. [PubMed: 22271394]

Patial S, Shahi S, Saini Y, Lee T, Packiriswamy N, Appledorn DM, Lapres JJ, Amalfitano A, Parameswaran N. G-protein coupled receptor kinase 5 mediates lipopolysaccharide-induced NFkappaB activation in primary macrophages and modulates inflammation in vivo in mice. Journal of Cellular Physiology. 2011; 226(5):1323–1333. [PubMed: 20945396]

Reuter G. The Lactobacillus and Bifidobacterium microflora of the human intestine: composition and succession. Curr Issues Intest Microbiol. 2001; 2(2):43–53. [PubMed: 11721280]

Riggs BL, Khosla S, Melton LJ 3rd. Sex steroids and the construction and conservation of the adult skeleton. Endocr Rev. 2002; 23(3):279–302. [PubMed: 12050121]

Roberfroid MB, Cumps J, Devogelaer JP. Dietary chicory inulin increases whole-body bone mineral density in growing male rats. The Journal of nutrition. 2002; 132(12):3599–3602. [PubMed: 12468594]

Sartor RB. Microbial influences in inflammatory bowel diseases. Gastroenterology. 2008; 134(2):577–594. [PubMed: 18242222]

Schaefer L, Auchtung TA, Hermans KE, Whitehead D, Borhan B, Britton RA. The antimicrobial compound reuterin (3-hydroxypropionaldehyde) induces oxidative stress via interaction with thiol groups. Microbiology. 2010; 156(Pt 6):1589–1599. [PubMed: 20150236]

Schloss PD, Westcott SL, Ryabin T, Hall JR, Hartmann M, Hollister EB, Lesniewski RA, Oakley BB, Parks DH, Robinson CJ, Sahl JW, Stres B, Thallinger GG, Van Horn DJ, Weber CF. Introducing mothur: open-source, platform-independent, community-supported software for describing and comparing microbial communities. Appl Environ Microbiol. 2009; 75(23):7537–7541. [PubMed: 19801464]

Scholz-Ahrens KE, Schrezenmeir J. Inulin and oligofructose and mineral metabolism: the evidence from animal trials. The Journal of nutrition. 2007; 137(11 Suppl):2513S–2523S. [PubMed: 17951495]

Shornikova AV, Casas IA, Isolauri E, Mykkanen H, Vesikari T. Lactobacillus reuteri as a therapeutic agent in acute diarrhea in young children. J Pediatr Gastroenterol Nutr. 1997; 24(4):399–404. [PubMed: 9144122]

Sjogren K, Engdahl C, Henning P, Lerner UH, Tremaroli V, Lagerquist MK, Backhed F, Ohlsson C. The gut microbiota regulates bone mass in mice. Journal of bone and mineral research : the official journal of the American Society for Bone and Mineral Research. 2012; 27(6):1357–1367.

Teitelbaum SL. Osteoclasts: what do they do and how do they do it? The American Journal of Pathology. 2007; 170(2):427–435. [PubMed: 17255310]

Thomas CM, Hong T, van Pijkeren JP, Hemarajata P, Trinh DV, Hu W, Britton RA, Kalkum M, Versalovic J. Histamine derived from probiotic Lactobacillus reuteri suppresses TNF via modulation of PKA and ERK signaling. PLOS One. 2012; 7(2):e31951. [PubMed: 22384111]

Thomas DW, Greer FR. Probiotics and prebiotics in pediatrics. Pediatrics. 2010; 126(6):1217–1231. [PubMed: 21115585]

Tubelius P, Stan V, Zachrisson A. Increasing work-place healthiness with the probiotic Lactobacillus reuteri: a randomised, double-blind placebo-controlled study. Environ Health. 2005; 4:25. [PubMed: 16274475]

Vaarala O, Atkinson MA, Neu J. The “perfect storm” for type 1 diabetes: the complex interplay between intestinal microbiota, gut permeability, and mucosal immunity. Diabetes. 2008; 57(10): 2555–2562. [PubMed: 18820210]

Valeur N, Engel P, Carbajal N, Connolly E, Ladefoged K. Colonization and immunomodulation by Lactobacillus reuteri ATCC 55730 in the human gastrointestinal tract. Appl Environ Microbiol. 2004; 70(2):1176–1181. [PubMed: 14766603]

Wang Q, Garrity GM, Tiedje JM, Cole JR. Naive Bayesian classifier for rapid assignment of rRNA sequences into the new bacterial taxonomy. Appl Environ Microbiol. 2007; 73(16):5261–5267. [PubMed: 17586664]

Weaver CM, Martin BR, Nakatsu CH, Armstrong AP, Clavijo A, McCabe LD, McCabe GP, Duignan S, Schoterman MH, van den Heuvel EG. Galactooligosaccharides improve mineral absorption and bone properties in growing rats through gut fermentation. J Agric Food Chem. 2011; 59(12):6501–6510. [PubMed: 21553845]

Weizman Z, Asli G, Alsheikh A. Effect of a probiotic infant formula on infections in child care centers: comparison of two probiotic agents. Pediatrics. 2005; 115(1):5–9. [PubMed: 15629974]

Wen L, Ley RE, Volchkov PY, Stranges PB, Avanesyan L, Stonebraker AC, Hu C, Wong FS, Szot GL, Bluestone JA, Gordon JI, Chervonsky AV. Innate immunity and intestinal microbiota in the development of Type 1 diabetes. Nature. 2008; 455(7216):1109–1113. [PubMed: 18806780]

Whelan K, Quigley EM. Probiotics in the management of irritable bowel syndrome and inflammatory bowel disease. Curr Opin Gastroenterol. 2013; 29(2):184–189. [PubMed: 23286925]

Yan F, Polk DB. Probiotics and immune health. Curr Opin Gastroenterol. 2011; 27(6):496–501. [PubMed: 21897224]

Yang LC, Wu JB, Lu TJ, Lin WC. The prebiotic effect of Anoectochilus formosanus and its consequences on bone health. Br J Nutr. 2012:1–10.

Yoo J, Tcheurekdjian H, Lynch SV, Cabana M, Boushey HA. Microbial manipulation of immune function for asthma prevention: inferences from clinical trials. Proceedings of the American Thoracic Society. 2007; 4(3):277–282. [PubMed: 17607013]

Zhao S, Zhang YK, Harris S, Ahuja SS, Bonewald LF. MLO-Y4 osteocyte-like cells support osteoclast formation and activation. J Bone Miner Res. 2002; 17(11):2068–2079. [PubMed: 12412815]

Non-standard Abbreviations

ATCC PTA	American type culture collection product test authorization
L. reuteri	Lactobacillus reuteri
TRAP5	tartrate resistant alkaline phosphatase 5
RANKL	receptor activator of NF-kB ligand
Ovx	ovariectomized
CD4	cluster of differentiation 4
μCT	microcomputed tomography
M-CSF	macrophage colony stimulating factor
TNF	tumor necrosis factor
BFR	bone formation rate
HPRT	Hypoxanthine guanine phosphoribosyl transferase
OC	osteocalcin
OPG	osteoprotegrin
OTU	operational taxonomic units

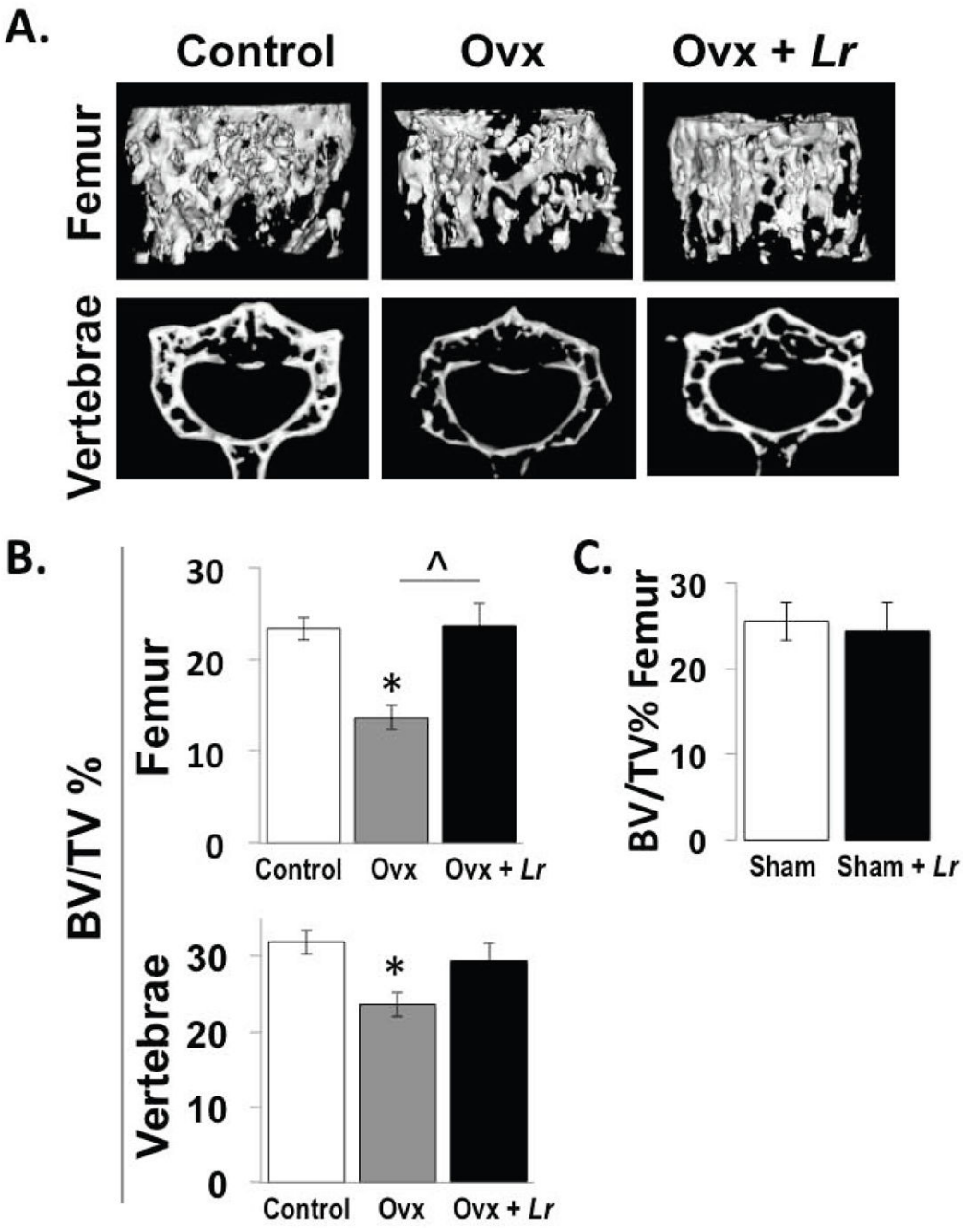

Figure 1. Ovariectomy (Ovx) mice treated with *L. reuteri* for 4 weeks display femur and vertebral trabecular bone volumes that are similar to ovary intact control mice

Representative micro-computed tomography isosurface images (*A*) and percent bone volume fraction (BV/TV) quantitative pooled data (*B, C*) obtained from the trabecular bone region of the distal femur and L3 vertebrae of non-Ovx control (white bar), Ovx (gray bar), and Ovx+*L. reuteri* treated (black bar) mice (A, B) and from sham versus sham plus L. reuteri treatment (C). *L. reuteri* was given by gavage only as described in the methods. Values are averages ± standard error, n=8 per group, * $p<0.05$ compared to Non-Ovx, ^ $p<0.05$ compared to Ovx as determined by one-way ANOVA followed by Tukey HSD.

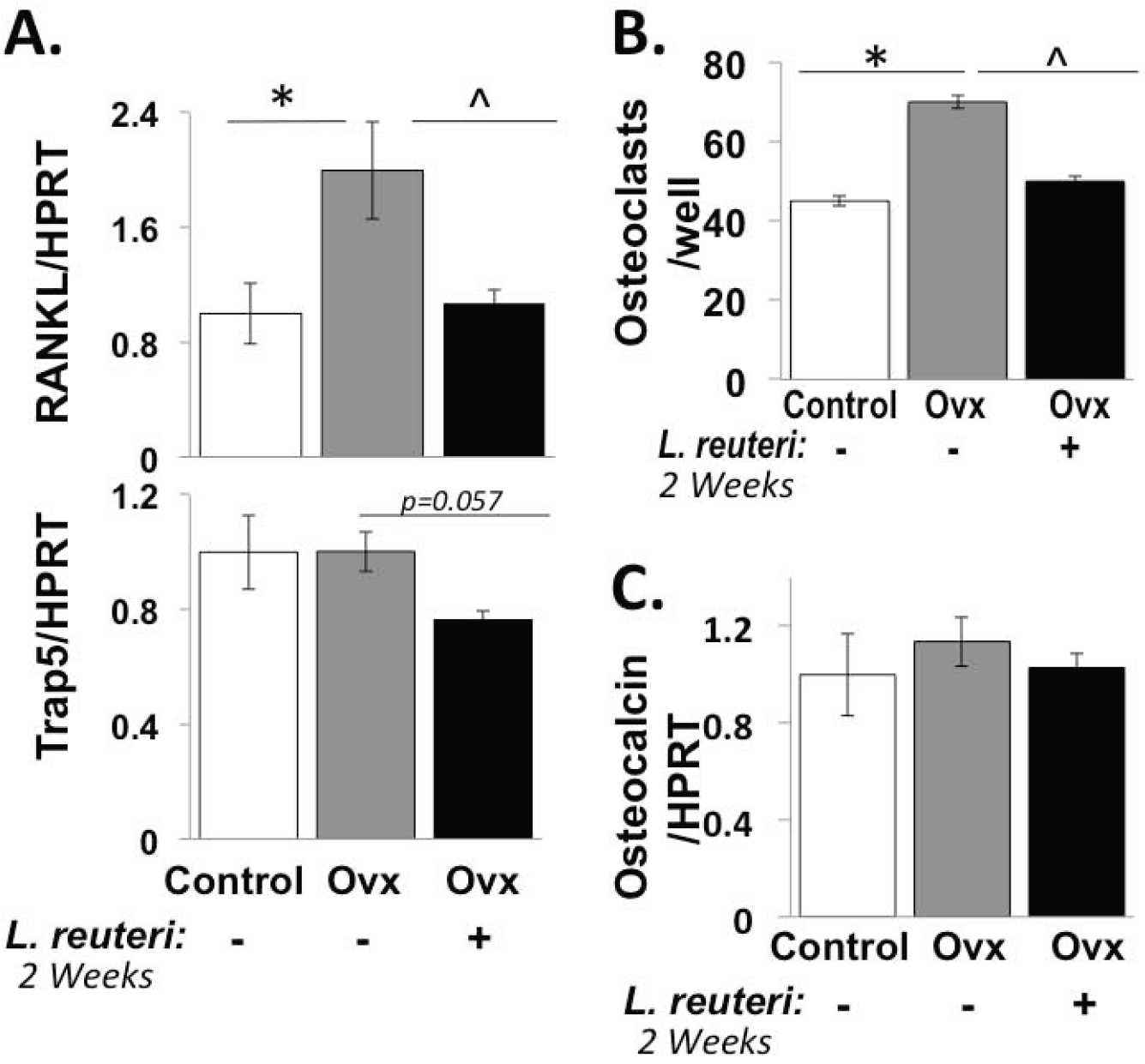

Figure 2. *L. reuteri* treatment prevents Ovx-induced increases in RANKL and bone marrow osteoclastogenesis after 2 weeks of probiotic treatment

Conditions are non-Ovx, intact mice (white bar); Ovx, ovariectomized mice (gray bar); Ovx + *Lr*, Ovx mice gavaged with *L. reuteri* for 2 weeks (black bar). (A) Levels of TRAP5 and RANKL RNA in whole tibia bone. Levels were expressed relative to HPRT, a non-modulated house-keeping gene. (B) Harvested mouse bone marrow cells from the mice above were cultured *in vitro* with RANKL and M-CSF and the number of osteoclasts counted per well. (C) Osteocalcin mRNA levels were measured in whole tibia bone and expressed relative to HPRT. Data values are average ± standard error, n ≥ 8 per group, * $p<0.05$ to Non-Ovx, ^ $p<0.05$ to Ovx by one-way ANOVA followed by Tukey HSD.

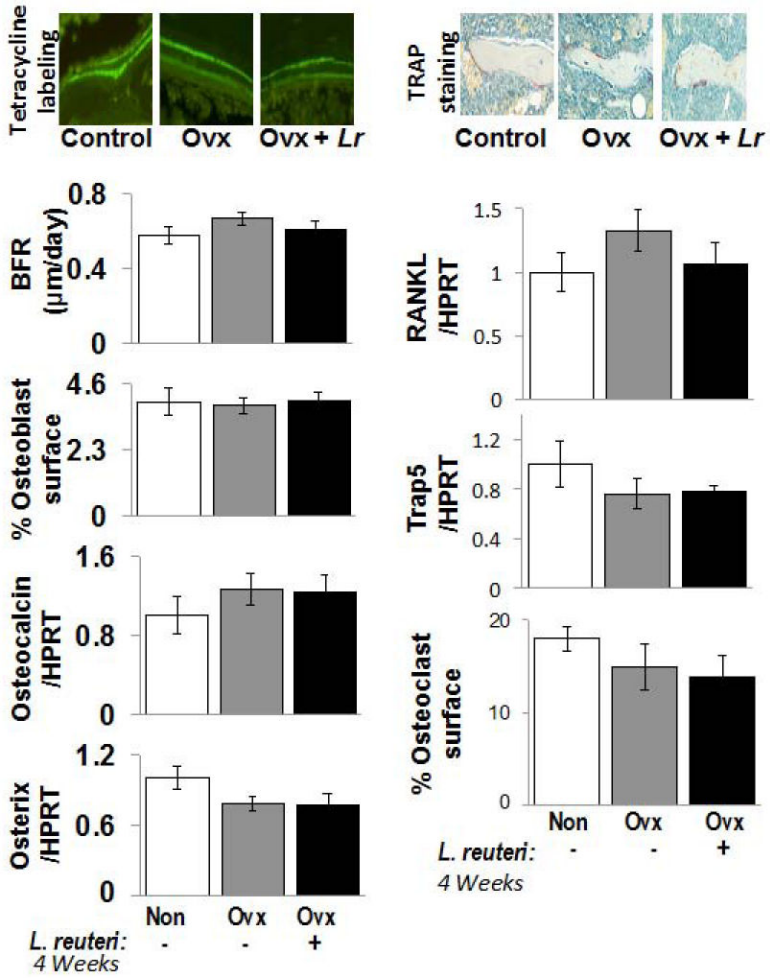

Figure 3. Osteoclast and osteoblast markers don't show significant changes in response to Ovx +/- *L. reuteri* treatment at 4 weeks

Top left: Representative fluorescent microscope photographs depicting the two pulses of calcein incorporation. The space between the two bands represents the mineral apposition rate (MAR). ***Top right:*** Representative microscope photographs of TRAP stained femur metaphyseal sections. Osteoclasts stain purple. ***Left Bar Graphs:*** Bone formation rate (BFR), osteoblast surface/total trabecular surface, and tibial RNA levels of osteocalcin and osterix (relative to HPRT an unaltered housekeeping gene). ***Right Bar Graphs:*** Tibial RNA levels of RANKL and Trap5 relative to HPRT, as well as osteoclast surface/total trabecular surface. Conditions are non-Ovx (white); Ovx, ovariectomized mice (gray); and Ovx + *Lr*, Ovx mice gavaged with *Lactobacillus reuteri* for 4 weeks (black). Values are averages ± standard error, n=8 per group, * $p<0.05$ to Non-Ovx by one-way ANOVA followed by Tukey HSD.

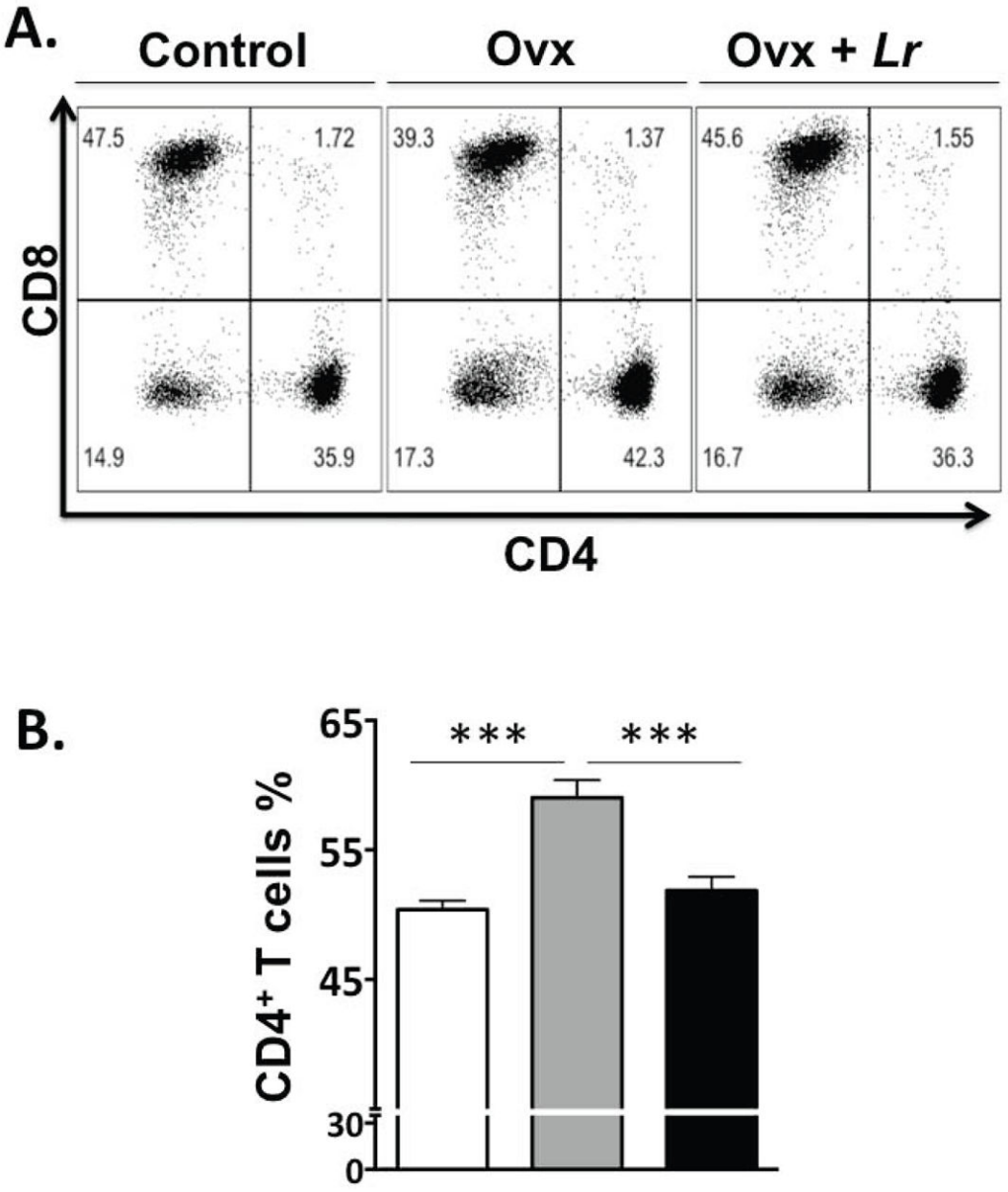

Fig 4. FACS analysis of bone marrow cells

Control, OVX and OVX+LR mice were treated as described and femurs collected during euthanasia at 2 weeks after treatment. Femurs were flushed and bone marrow cells were collected, processed and stained for cell surface markers for identifying the various immune cells as described in the methods. $CD4^+$ T-lymphocytes were identified as $CD3^+CD4^+$ T-cells; Dot plots are shown at the top and cumulative data presented in graph in the bottom. In the dot plots, the numbers in the quadrants indicate the percentage of cells. N=8 for each condition; ***P<0.001 as determined by ANOVA followed by Bonferroni.

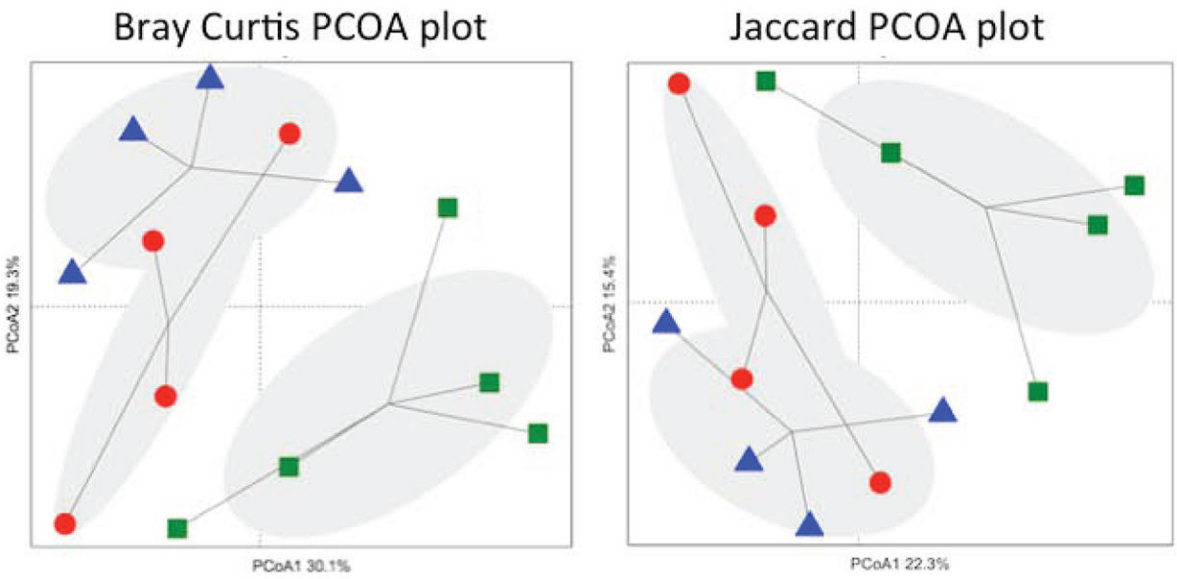

Figure 5. Two-dimensional projection of the principal coordinate analysis (PCoA) of bacterial 16S sequences from mouse jejunum samples along the first two principal axes

Left. PCoA was calculated using the Bray-Curtis similarity measures (coordinate axis 1 percent variation explained=30.1%, coordinate axis 2=19.3%). ***Right.*** PCoA was calculated using the Jaccard similarity measure (coordinate axis 1 percent variation explained=22.3%, coordinate axis 2=15.4%). Non-OVX mice (▲), OVX mice (●), *L.reuteri*-treated OVX mice (■).

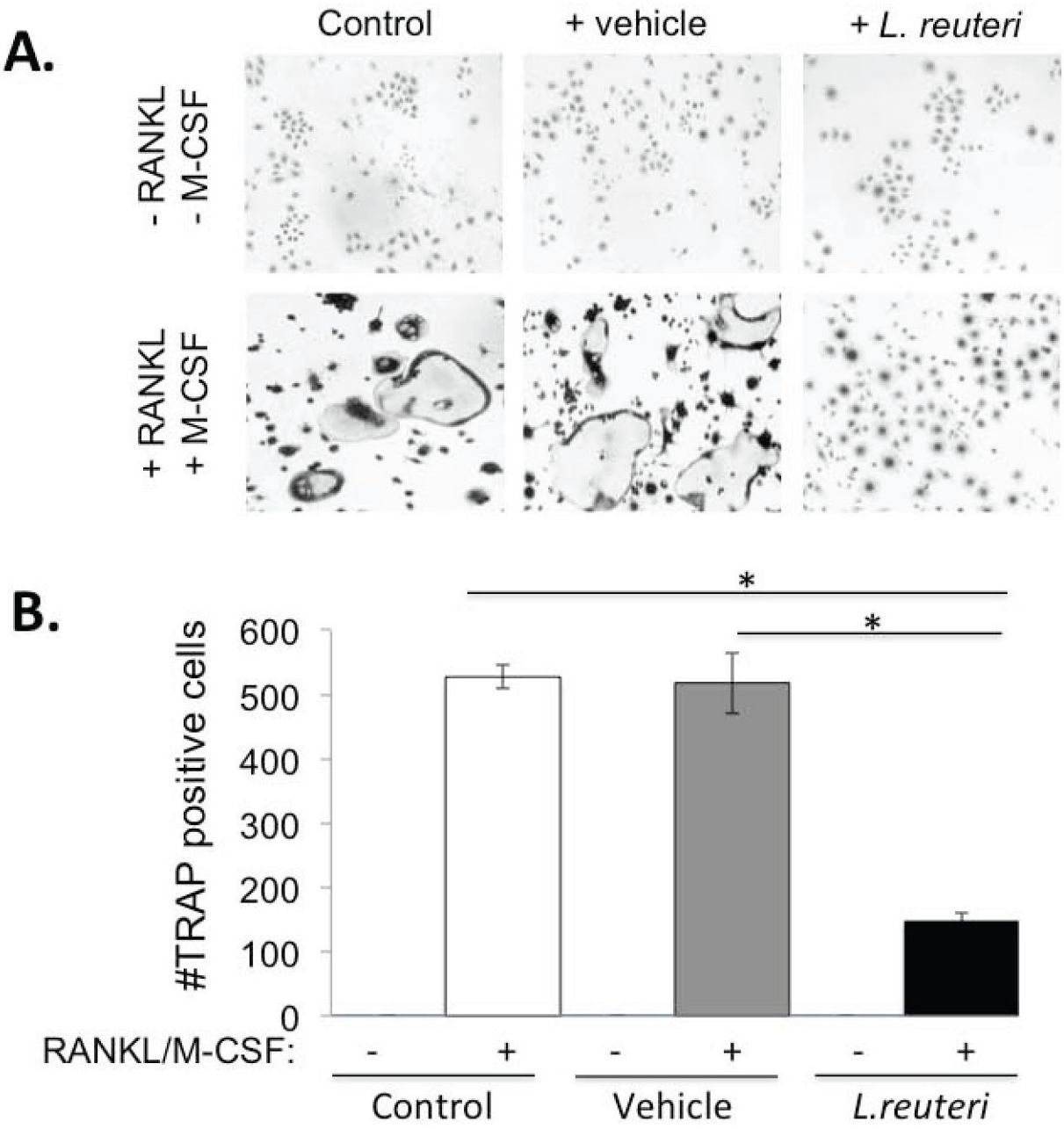

Figure 6. Effect of *L. reuteri* secreted factors on osteoclast differentiation in Raw 264.7 cells

(*A*) Representative images of TRAP$^+$ multinuclear giant cells at 7 days after RANKL and M-CSF treatment. (a) Cells only (Negative control) (b) RANKL and M-CSF (Positive control) (c) MEM-α (d) MEM-α plus RANKL and M-CSF (e) *L. reuteri* conditioned MEM-α (LR CM) (f) LR CM plus RANKL and M-CSF. (*B*) Quantification of TRAP$^+$ multinuclear (>3 nuclei/cell) giant cells at 7 days after treatment with RANKL (100ng/ml) and M-CSF (10ng/ml) per visual field under light microscopy. Values are averages ± standard deviations. Conditions were done in triplicate and the entire experiment repeated 4 times. * $p < 0.05$ by Students t-test.

Table 1

Femur Bone Parameters

	Non-Ovx	Ovx	Ovx+*Lr*
Trabecular			
BV/TV	23.3 ± 1.2	13.6 ± 1.3 *	23.6 ±2.5 ^
BMD (mg/cc)	230 ± 6	179 ± 7 *	222 ± 11 ^
BMC (mg)	0.38 ± 0.02	0.27 ± 0.01 *	0.35 ± 0.02 ^
Tb. Th. (μm)	45.4 ± 1.2	35.8 ± 2.2 *	41.3 ± 1.9
Tb. N. (1/mm)	5.14 ± 0.24	3.80 ± 0.29	5.66 ± 0.50 ^
Tb. Sp. (μm)	152 ± 10	234 ± 20 *	145 ± 17 ^
Cortical			
Tt. Ar. (mm^2)	1.53 ± 0.03	1.46 ± 0.02	1.49 ± 0.04
Ct. Ar. (mm^2)	0.97 ± 0.03	0.88 ± 0.01	0.93 ± 0.03
Ma. Ar. (mm^2)	056 ± 0.01	0.58 ± 0.01	0.56 ± 0.01
Ct Ar/Tt. Ar.	0.63 ± 0.01	0.60 ± 0.01	0.62 ± 0.01
Thickness (mm)	0.27 ± 0.01	0.25 ± 0.01	0.27 ± 0.01
Inner P. (mm)	2.83 ± 0.02	2.86 ± 0.04	2.80 ± 0.02
Outer P. (mm)	4.54 ± 0.04	4.44 ± 0.04	4.47 ± 0.06

Femur distal trabecular bone and diaphyseal cortical bone parameters. Non-Ovx, intact mice; Ovx, ovariectomized; Ovx+*L.r.*, Ovx mice treated with *Lactobacillus reuteri*. BV/TV, bone volume fraction; BMD, bone mineral density; BMC, bone mineral content; Tb. Th., trabecular thickness; Tb. N., trabecular number; Tb. Sp., trabecular spacing; Tt. Ar., total area; Ct. Ar., cortical area; Ma. Ar., marrow area; Ct. Ar./Tt. Ar., cortical area fraction; Inner P., inner perimeter; Outer P., outer perimeter. Data are averages ± standard error, n=8 per group,

* $p<0.05$ to Non-Ovx,

^ $p<0.05$ to Ovx by one-way ANOVA followed by Tukey HSD.

Table 2

Vertebrae Bone Parameters

	Non-Ovx	Ovx	Ovx+*Lr*
Trabecular			
BMD (mg/cc)	218 ± 8	182 ± 8 *	204 ± 10
BMC (mg)	0.36 ± 0.01	0.29 ± 0.01 *	0.36 ± 0.01
Tb. N. (1/mm)	6.72 ± 0.19	6.24 ± 0.31	7.17 ± 0.35
Tb.Th. (μm)	47.4 ± 1.81	37.5 ± 1.00 *	40.8 ± 1.48 *
Tb. Sp. (μm)	102 ± 5	126 ± 9	100 ± 7

Vertebrae distal trabecular bone parameters.Non-Ovx, intact mice; Ovx, ovariectomized; Ovx+*L.r*., Ovx mice treated with *Lactobacillus reuteri*. BV/TV, bone volume fraction; BMD, bone mineral density; BMC, bone mineral content; Tb. Th., trabecular thickness; Tb. N., trabecular number; Tb. Sp., trabecular spacing; Data are averages ± standard error, n=8 per group,

* $p<0.05$ to Non-Ovxby one-way ANOVA followed by Tukey HSD.

Table 3

Beta diversity analysis

Distance metric	Comparison	R Value (*p value*)
Bray-Curtis	wtbroth-ovxbroth-ovxlacto	0.3393 (*0.0176*) *
	wtbroth-ovxbroth	0.05382 (*0.3106*)
	wtbroth-ovxlacto	0.5979 (*0.0246*) *
	ovxbroth-ovxlacto	0.3448 (*0.0629*)
Jaccard	wtbroth-ovxbroth-ovxlacto	0.5344 (*0.0005*)*
	wtbroth-ovxbroth	0.1736 (*0.2751*)
	wtbroth-ovxlacto	0.8094 (*0.0076*)*
	ovxbroth-ovxlacto	0.4938 (*0.0100*)*

Diversity in jejunal tissue was assessed and analyzed by ANOSIM. Subsampling cutoff = 374 sequences.

* Indicates statistical significance